Exploring the dynamics of astaxanthin production in Haematococcus pluvialis biofilms using a rotating biofilm-based system

David Morgado, Andrea Fanesi, Thierry Martin, Sihem Tebbani, Olivier Bernard, Filipa Lopes

Received: 4 October 2023 | Revised: 27 November 2023 | Accepted: 5 December 2023

DOI: 10.1002/bit.28624

ARTICLE

BIOTECHNOLOGY AND BIOENGINEERING WILEY

Exploring the dynamics of astaxanthin production in *Haematococcus pluvialis* biofilms using a rotating biofilm-based system

David Morgado[1] | Andrea Fanesi[1] | Thierry Martin[1] | Sihem Tebbani[2] | Olivier Bernard[3] | Filipa Lopes[1]

[1]CentraleSupélec, Laboratoire Génie des Procédés et Matériaux (LGPM), Université Paris-Saclay, Gif-sur-Yvette, France

[2]CentraleSupélec, CNRS, Laboratoire des Signaux et Systèmes (L2S), Université Paris-Saclay, Gif-sur-Yvette, France

[3]INRIA, Centre d'Université Côte d'Azur, Biocore, CNRS, Sorbonne Université, Sophia-Antipolis, France

Correspondence
Andrea Fanesi, CentraleSupélec, Laboratoire Génie des Procédés et Matériaux (LGPM), Université Paris-Saclay, Gif-sur-Yvette, France.
Email: andrea.fanesi@centralesupelec.fr

Funding information
European Union's Horizon 2020 Research and Innovation Program, Grant/Award Number: 955520

Abstract

Microalgae biofilm emerged as a solid alternative to conventional suspended cultures which present high operative costs and complex harvesting processes. Among several designs, rotating biofilm-based systems stand out for their scalability, although their primary applications have been in wastewater treatment and aquaculture. In this work, a rotating system was utilized to produce a high-value compound (astaxanthin) using *Haematococcus pluvialis* biofilms. The effect of nitrogen regime, light intensity, and light history on biofilm traits was assessed to better understand how to efficiently operate the system. Our results show that *H. pluvialis* biofilms follow the classical growth stages described for bacterial biofilms (from adhesion to maturation) and that a two-stage (green and red stages) allowed to reach astaxanthin productivities of 204 mg m^{-2} d^{-1}. The higher light intensity applied during the red stage (400 and 800 µmol m^{-2} s^{-1}) combined with nitrogen depletion stimulated similar astaxanthin productivities. However, by training the biofilms during the green stage, using mild-light intensity (200 µmol m^{-2} s^{-1}), a process known as priming, the final astaxanthin productivity was enhanced by 40% with respect to biofilms pre-exposed to 50 µmol m^{-2} s^{-1}. Overall, this study shows the possibility of utilizing rotating microalgae biofilms to produce high-value compounds laying the foundation for further biotechnological applications of these emerging systems.

KEYWORDS
astaxanthin, elemental composition, FTIR-spectroscopy, *Haematococcus pluvialis*, microalgae biofilms, priming

1 | INTRODUCTION

Microalgae farming, recognized for its applications within the blue economy and its role in climate change mitigation, currently occupies a small niche in the global market (van Duinen et al., 2023). The primary constraint in expanding microalgae production lies in the complexity of scaling up cultivation facilities to meet industrial demands. This includes challenges from the inoculation of the cultivation system to the maintenance of a stable culture until the extraction and purification of bioproducts. There are various

cultivation systems available for microalgae production, from open ponds to closed photobioreactors. Yet, the minimal productivity benefits of one system over another are often outweighed by the overall costs of the cultivation process. Expenses arising from energy and water inputs, coupled with low biomass concentration and further costs in downstream processing, hinder microalgae farming from being economically sustainable (Khan et al., 2018; Moreno-Garcia et al., 2017).

Biofilm-based cultivation systems have emerged in response, presenting a more efficient solution with reduced water use, simplified harvesting processes, and improved light availability, as reviewed by Mantzorou and Ververidis (2019) and Moreno Osorio et al. (2021). Various algal biofilm cultivation strategies are in place, including submerged, intermittently submerged, and perfused systems (Berner et al., 2015). Depending on their specific design, these systems can be static, such as in porous substrate bioreactors (PSBRs) (Podola et al., 2017), or dynamic, like rotating biofilm-based systems (Bernard et al., 2015; Christenson & Sims, 2012; Gross et al., 2013).

Life-cycle analyses (LCAs) have already highlighted their economic advantages compared to open raceway systems, where rotating biofilm-based systems can reduce energy and water consumption by approximately 55% and 30%, respectively (Morales et al., 2020). These systems have been so far mainly used in wastewater treatment (Elystia et al., 2023; Gross-Wen Technologies, 2014; Kesaano & Sims, 2014) and aquaculture (Inalve, 2016), leaving their potential for producing high-value compounds largely unexplored (Wood et al., 2022).

Given the prohibitive costs associated with microalgae industrial production, there is a pressing focus on targeting markets for aquaculture feed and specialty chemicals in nutraceuticals, pharmaceuticals, and cosmetics (van Duinen et al., 2023). Among these, astaxanthin emerges as a molecule of interest. Large-scale facilities around the world produce astaxanthin by cultivating *Haematococcus pluvialis* as a two-stage process based on its life cycle and cell biology: the green stage focuses on cell multiplication and growth, while the red stage targets astaxanthin accumulation under stress conditions (e.g., high light and low nutrients) (Li et al., 2020).

Although PSBR technology has been used with *H. pluvialis*, such systems are difficult to scale up (Podola et al., 2017). Also, a more in-depth comprehension of how cells undergo the different stages of biofilm formation is needed to improve operational efficiency. It is worth noting that since *H. pluvialis* activates its astaxanthin biosynthetic pathway under stress, training the cells to better withstand the triggering period could be an interesting area of unexplored research, especially within a biofilm context. In this respect, pre-exposing cells to a mild stress, a process known as priming (Conrath et al., 2006), may be utilized to gain faster or higher levels of astaxanthin. Indeed, cells pre-exposed to unfavorable conditions might have the metabolic machinery ready to respond to a new stress event. This approach has been already investigated from an ecological point of view (Jueterbock et al., 2021), in several microorganisms (Andrade-Linares et al., 2016), and in plants for crop production (Liu et al., 2022).

In this study, we investigated the production of astaxanthin using the classical two-stage process in a rotating biofilm-based system, with *H. pluvialis* biofilms grown on cotton carriers. The pre-exposition of the biofilm to different light intensities (priming) was investigated as a possible enhancer of astaxanthin productivity. An in-depth characterization of biomass and astaxanthin productivity was conducted and the biofilm dynamics were studied at different scales of resolution. A microscopic evolution of the biofilms on cotton carriers was investigated using confocal laser scanning microscopy, and changes in macromolecular and elemental composition were followed to elucidate the acclimation mechanisms in *H. pluvialis* biofilms.

2 | MATERIALS AND METHODS

2.1 | Planktonic culture maintenance

H. pluvialis CCAC 0125 from the Central Collection of Algal Cultures (CCACs) at the University of Duisburg-Essen (UDE) Cologne, Germany, was grown in continuous mode in 3N-Bristol medium (Nichols & Bold, 1973) in a chemostat of 2-L working volume at a dilution rate of $0.3\,d^{-1}$. The reactor was illuminated with a photosynthetic photon flux density (PPFD) of $80\,\mu mol\,m^{-2}\,s^{-1}$ of continuous light, bubbled with air, and mixed using a magnetic stirrer. The pH of the culture was regulated at 7.0 ± 0.1 by automatically adding CO_2 to the airflow using a pH controller (JBL Proflora CO_2 controller).

The continuous culture was used to prepare two batch reactors (2-L each) that were grown for 7 days (final biomass concentration of $0.75\,g\,L^{-1}$) and used as inoculum for the rotating biofilm system. The batch reactors were grown under the same conditions described above.

2.2 | Rotating biofilm-based system

The design of the rotating biofilm system used in this study is reported in Figure 1. Each cylinder was covered with 18 rectangular 100% cotton carriers ($250\,g\,m^{-2}$), with an average area of $22\,cm^2$, used for biofilm growth. The cotton carriers were fixed on the cylinder by silicone tubes of 1.3 mm in diameter. After the system was assembled, the cylinders and the cotton carriers were chemically sterilized for 4 h, with a 9:1 (v:v) mixture of de-ionized water and a mixture of hydrogen peroxide and peracetic acid (Contec™ PeridoxRTU). The system was then rinsed overnight, in batch operation, with de-ionized sterile water.

The inoculum was performed by filling each PP container with 1 L of the 7-day batch cultures. This volume ensured that half of each cylinder was submerged in the medium, to maintain the same exposure over time of the cotton carriers to the growth medium and to light and darkness cycles. The pH of each reactor was regulated at 7.0 ± 0.1 by automatically adding CO_2 to the container using a pH

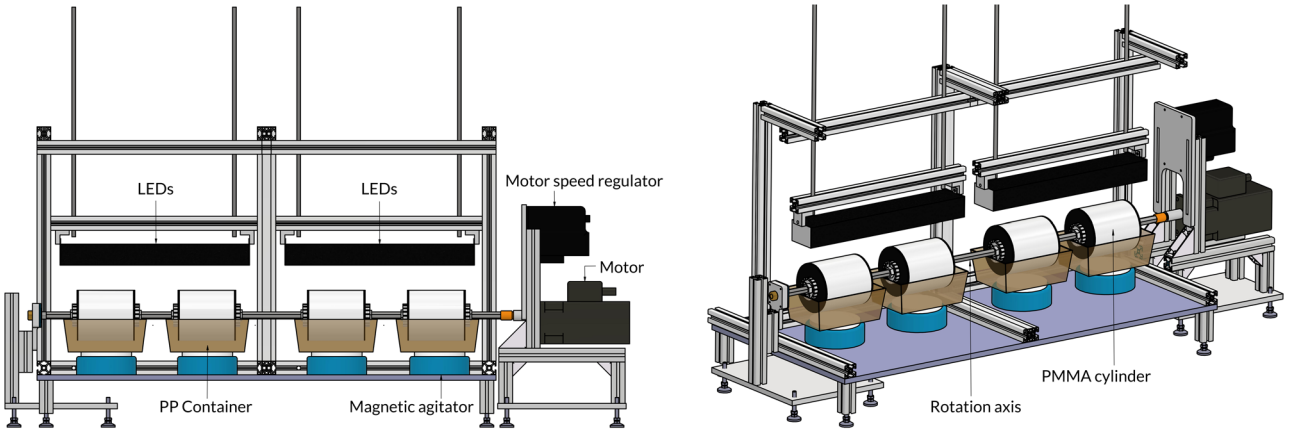

FIGURE 1 Schematics of the design of the rotating biofilm system. It consisted of a motor and a stainless steel axis of 1.20 m length, on which four reactors were assembled. Each reactor consisted of a 1-L polypropylene (PP) container equipped with a 110 mm diameter × 125 mm length poly(methyl methacrylate) (PMMA) cylinder. The four cylinders were mounted on a rotating 90 W motor (Panasonic M9M), operated at a linear velocity of 0.0346 m s^{-1} (6 rpm). Each PP container was placed on a stirring platform that ensured continuous mixing.

controller. Continuous illumination with photosynthetically active radiation (PAR) was provided by a 48 W system (Alpheus led, France) equipped with 16 red, 7 blue, and 7 white LEDs on the top surface of each cylinder. The temperature was maintained at an average of 22 ± 1°C (room-controlled).

2.3 | Experimental design

A set of experiments was carried out to determine the conditions under which astaxanthin accumulation in the biofilms could be triggered by varying nutrient and light levels, simulating a two-stage cultivation method (biomass growth or green stage and astaxanthin production or red stage). The system consisted of four independent reactors, allowing for the assessment of multiple conditions in parallel. Each experiment was conducted over a period of 15 days, divided into two stages.

During the first 7 days of each experiment, all reactors were maintained under replete nitrogen conditions—green stage. Two reactors were exposed to a PPFD of 50 µmol m^{-2} s^{-1}, while the other two were exposed to a PPFD of 200 µmol m^{-2} s^{-1}. After 7 days, the light intensity was increased in all reactors to a fixed level of either 400 or 800 µmol m^{-2} s^{-1}. At this point, the medium of the two reactors was changed to a nitrogen-deplete condition (N-deplete)—red stage, while the other two were maintained under replete nitrogen conditions (N-replete). The nitrogen-depleted medium was prepared by removing $NaNO_3$.

Samples were taken at regular intervals throughout the 15-day experiment at Days 0 (after 4 h from the inoculum), 1, 2, 4, 5, 7, 8, 9, 11, 12, and 15. Biofilm morphology, structure, and cell distribution on the cotton carriers were observed at macroscopic and microscopic scales. Biofilm traits such as biomass and cell areal densities, pigments as well as elemental composition and macromolecular pools were quantified.

2.4 | Sample preparation

Differently from other studies on rotating biofilm-based systems, where biomass growth is followed by repeated harvest and regrowth cycles (Blanken et al., 2014; Mousavian et al., 2023), for each sampling point, one cotton carrier was collected from each reactor. The cotton carrier was placed in 50 mL tubes and the biofilm was removed with de-ionized water using multiple vortex steps until all biomass was re-suspended. The total volume of the suspended biofilm (V_{total}) was recorded and aliquots from the algal suspension were used for the following measurements.

2.5 | Biomass and cell areal densities

Whatman glass microfiber filters (d = 47 mm) were pre-dried at 100°C. The empty filters (W_F) were weighted, and a determined volume (V_{DW}) of suspended biofilm was filtrated under vacuum (5–10 mL depending on the growth stage). The wet filters with biomass (W_B) were dried at 100°C overnight and weighed. The area (A_c) was determined by image analysis on ImageJ (Schneider et al., 2012) from pictures of the cotton carriers. The biomass areal density (g m^{-2}) of the samples was then calculated according to Equation (1):

$$\text{Biomass areal density(g m}^{-2}) = \frac{W_B - W_F}{V_{DW}} \times V_{total} \times \frac{1}{A_c}. \quad (1)$$

Cell number (N) (cell mL^{-1}) was determined using a Guava EasyCyte HT flow cytometer (Luminex). Aliquots of the suspended biofilm were diluted up to 10 times (D_f) to obtain samples with cell concentrations around 200 cells $µL^{-1}$. Measurements were based on a combination of forward scatter (FSC) and side scatter (SSC), in conjunction with chlorophyll fluorescence. Chlorophyll *a* was excited at 488 nm, and its fluorescence was detected at 680 nm. Chlorophyll a was excited at

488 nm and fluorescence was detected at 680 nm. The cell areal density (cells m^{-2}) was then calculated according to Equation (2):

$$\text{Cell areal density (cells } m^{-2}) = N \times D_f \times V_{\text{total}} \times \frac{1}{A_c}. \quad (2)$$

2.6 | Astaxanthin and chlorophyll quantification

Pigments were extracted using dimethyl sulfoxide (DMSO, >99.9%, Thermo Fisher Scientific) in a water bath at 70°C for 10 min. Astaxanthin content was measured spectrophotometrically at 530 nm (Evolution 60S UV-visible spectrophotometer, Thermo Fisher Scientific), to avoid the interference of other carotenoids, as described by Li et al. (2012). Chlorophylls *a* and *b* were determined at 649 and 665 nm, as described by Wellburn (1994). Respective equations are described in Supporting Information (Figure S1 and Equations S1, S2, and S3). Total chlorophyll content, calculated as the sum of chlorophylls *a* and *b*, and astaxanthin content, were calculated as milligrams per gram of dry weight (% of DW). Subsequent estimation of both pigments per areal density (g m^{-2}) was obtained by multiplying the pigments content with the respective biomass areal density.

2.7 | Biomass and astaxanthin productivity

Biomass and astaxanthin productivities (g m^{-2} d^{-1}) were calculated according to Equation (3):

$$\text{Productivity (g } m^{-2} \text{ } d^{-1}) = \frac{X_{t+i} - X_t}{\Delta t}, \quad (3)$$

where x_t represents biomass or astaxanthin areal densities obtained at time t and x_{+i} represents biomass or astaxanthin areal densities obtained after the interval of time i. Δt is the interval of time $(t + i)-t$.

2.8 | ATR-FTIR spectroscopy

The macromolecular composition of the biofilm was analyzed using an ATR-FTIR PerkinElmer Spectrum-two Spectrometer (PerkinElmer). Aliquots of the suspended biofilm were centrifuged at 7000*g* for 1 min and washed two times. About 2 µL of a concentrated sample was transferred on a 45° ZnSe crystal and dried for 20 min. The empty crystal was measured as a background before loading the algal samples. Infrared spectra were recorded in the range of 4000–400 cm^{-1} using an accumulation of 16 scans with a spectral resolution of 4 cm^{-1}. The spectra were baselined and the maximum absorption values in the spectral ranges of carbohydrates (C–O–C; 1200–950 cm^{-1}), lipids (C=O vibration; 1770–1720 cm^{-1}), and proteins (Amide I; 1700–1630 cm^{-1}) were used to estimate the ratios between these macromolecular pools (lipids to proteins, carbohydrates to proteins and carbohydrates to lipids) (Fanesi et al., 2019).

2.9 | CHNS

The carbon, nitrogen, hydrogen, and sulfur content of the biofilm samples (1–2 mg of dried biomass) was determined using an Elemental Analyzer (Organic Elemental Analyzer FLASH 2000 CHNS/O, Thermo Fisher Scientific).

2.10 | Biofilm imaging

The macroscopic coverage of the cotton carriers was captured using a smartphone camera, and pictures (3000 × 4000 pixels) were taken under similar illumination conditions. The microscopic structure of the biofilms was observed using a confocal laser scanning microscope (CLSM). CLSM images (1536 × 1536 pixels) were acquired using an inverted Zeiss LSM700 confocal microscope (Carl Zeiss Microscopy GmbH) and 10× (0.25 N.A.) objective. Voxel size was 2.5 × 2.5 × 7 μm^3 and each image covered an area of 3.8 × 3.8 mm^2. Microalgae cells were observed by detecting chlorophyll *a* autofluorescence (ex. 639 nm).

2.11 | Statistics

Statistics were performed using Python 3.9.13. Two-way ANOVA was used to test the statistical significance of mean differences among different light conditions and over time. The level of significance was always set at 5%. All results are reported as mean and standard deviations of several independent biological replicates (see Table 1 in Section 3 for number of replicates). All layouts were generated in Inkscape 1.3 (Harrington et al., 2003).

TABLE 1 Biofilm and carotenogenesis stages: adhesion, green stage low light (Green-LL), green stage high light (Green-HL), and red stage high light (Red-HL).

Stage	N-condition	Days		Light history	Light intensity	*n*
Adhesion	N-replete	0	2	—	50	7[a]
					200	
Green-LL	N-replete	4	7	—	50	8
					200	
Green-HL	N-replete	8	15	50	400	4
				200		4
Red-HL	N-deplete	8	15	50	800	4
				200		4

Note: n refers to the number of replicates for each stage.
[a]For the adhesion stage, one sample was lost due to an experimental problem.

3 | RESULTS

3.1 | *H. pluvialis* biofilm development under rotating conditions

Our data clearly demonstrated that *H. pluvialis* biofilm growth dynamics are markedly influenced by nutrient availability and light intensity. Four main stages were identified and are reported in Table 1.

For the first time, the evolution of the life-cycle stages of *H. pluvialis* during biofilm development was described (Figure 2). An increase in surface coverage and a shift from small to bigger cells could be observed from Days 0 to 7 (Figure 2B,C). Interestingly, after Day 7, once the biofilms were subjected to higher light intensity

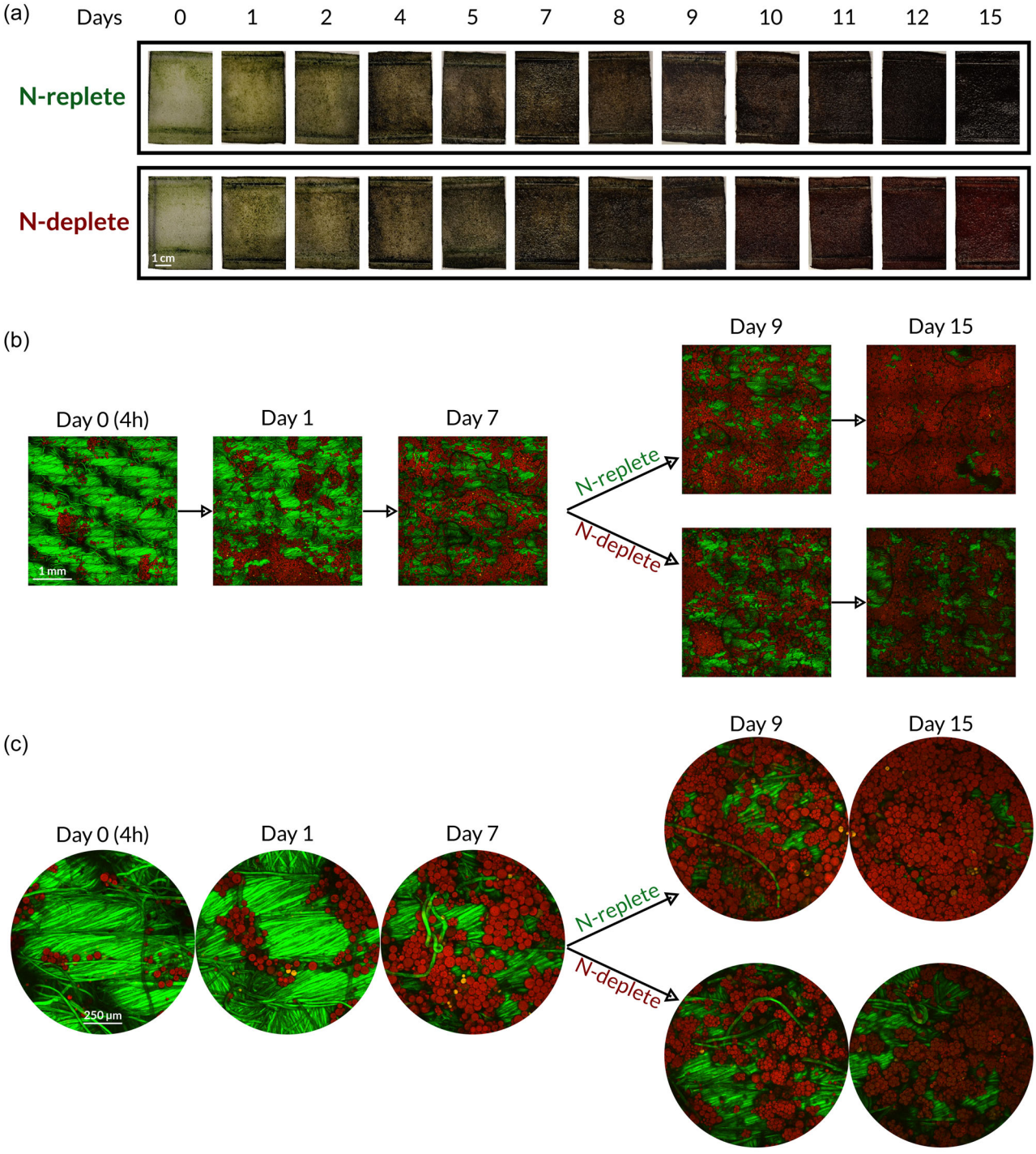

FIGURE 2 *Haematococcus pluvialis* biofilm development on cotton carriers at the macroscopic and microscopic scale. In panel (a), images of the cotton carriers colonized by the biofilms in the presence and absence of nitrogen are reported. Panel (b) depicts the microscopic spatial organization of *H. pluvialis* biofilms on the cotton fibers, whereas in (c), representative zoom is reported to highlight morphological changes of *H. pluvialis* cells and colonies. All images are *Z*-projections of 3D stacks obtained using a confocal laser scanning microscope. The autofluorescence of chlorophyll *a* is reported in red, whereas the cotton fibers are in green. Brightness and contrast were adjusted for visualization purposes.

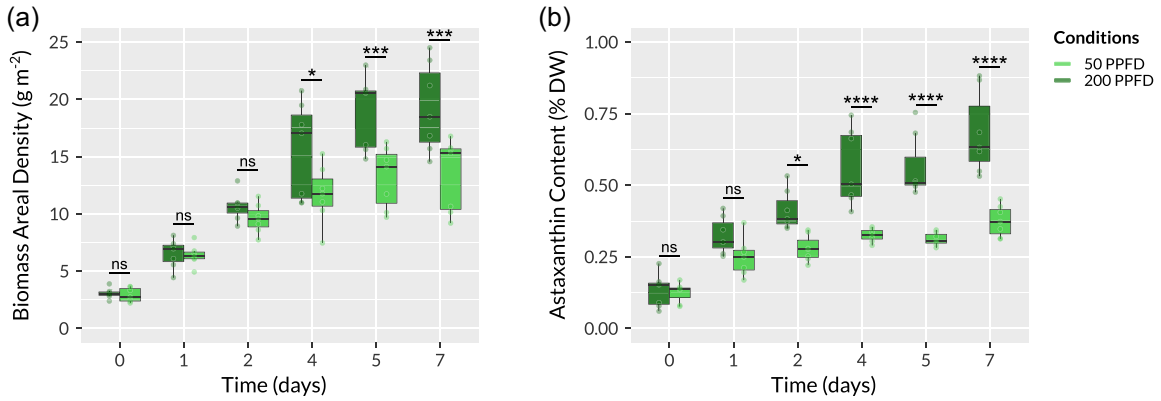

FIGURE 3 Dynamics of *Haematococcus pluvialis* during the adhesion and green stages exposed to a photosynthetic photon flux density (PPFD) of either 50 (light green) or 200 µmol m^{-2} s^{-1} (dark green). (a) Biomass areal density (g m^{-2}) and (b) astaxanthin content (as % dry weight) ($n = 7$). Statistically significant differences between PPFDs are represented by the asterisks (*$p < 0.05$, ***$p < 0.005$, ****$p < 0.0005$), and were determined using a two-way ANOVA analysis.

(PPFD of 400 or 800), cells formed palmelloid aggregates characterized by the presence of groups of 8–32 cells. As expected, the cell cycle also changed with the nitrogen regime. Under N-deplete conditions, the palmelloid aggregates remained prominent but there was no discernible increase in the number of cells or in the surface coverage. Conversely, in N-replete, the cotton carriers were completely covered, but the biofilm was represented mainly by single larger cells, closely mirroring the observations from Day 7. No evidence of the palmelloid aggregates was visible.

Morphological changes at the cell and biofilm scales were accompanied by important adjustments in biomass, pigments, and macromolecular contents in response to light intensity and nutrient concentration. Upon inoculation, planktonic cells displayed an initial adhesion to the cotton carrier, noticeable already after 4 h. Interestingly, no significant difference in biomass areal density until Day 2 was observed as a function of light (Figure 3a) ($p > 0.05$). This light-independent adhesion registered a rate of 3.5 ± 0.8 g m^{-2} d^{-1} (calculated between Days 0 and 2, for both 50 and 200 PPFD). After the adhesion stage, biomass accumulation on the cotton carriers slowed down, reaching a *plateau* under both light intensities. Notably, at the *plateau*, the biofilms exposed to PPFD of 200 exhibited both higher biomass areal density (44%) and astaxanthin content (81%) compared to those at PPFD of 50 ($p < 0.05$) (Figure 3).

After Day 7, higher light intensity (PPFD of 400 or 800) led to an increase in biomass areal density in both nitrogen conditions. In the N-replete biofilms, by Day 15, there was a fourfold increase, and the biomass areal density was found to be 17% higher at a PPFD of 800 compared to 400 (Figure 4a). On the other hand, in terms of pigment content, macromolecular, and elemental compositions, no significant fluctuations were observed. Total chlorophyll represented around 1.6% of dry weight, while astaxanthin remained under 1.1% (Figure 5). Steady internal quotas (Supporting Information: Table S1) were also observed for both carbon (46%) and nitrogen (6.3%), yielding a C:N ratio of approximately 7.3. The lipids to proteins ratio also remained consistently below 0.2 (Figure 6c).

Under N-deplete conditions, although biomass increased from Days 7 to 15, the cell areal density remained unchanged (Figure 4d and Supporting Information: Figure S2). As a result, cell weight tripled by Day 11, leveling off at the end of the experiment, and was double that observed in N-replete cells (Figure 4f and Supporting Information: Figure S2). The C:N ratio increased 2.7-fold and 2-fold (Figure 6a), and the lipids to proteins ratio increased 2-fold and 3-fold at PPFD of 400 and 800, respectively (Figure 6c). Regardless of the light intensity, the cells exhibited an eightfold increase in astaxanthin content, reaching up to 3.5% of dry weight (Figure 5d), while total chlorophyll was reduced threefold from 1.8%–0.6% of dry weight (Figure 5b).

3.2 | Light history effect on *H. pluvialis* biofilm astaxanthin production

While both nitrogen and light intensity markedly impacted biofilm traits and life cycles, light history in itself turned out to play a key role. This effect was especially pronounced under N-deplete biofilms.

Pre-exposure to a PPFD of 200 instead of 50, enhanced growth metrics such as biomass and cell areal densities, regardless of the subsequent light intensities (either 400 or 800, Figure 4). In contrast, astaxanthin content remained unchanged. Therefore, astaxanthin productivity of the biofilms previously exposed to 200 PPFD was boosted by 37% and 41% at PPFD of 400 and 800, respectively ($p < 0.05$) (Figure 7).

4 | DISCUSSION

4.1 | Rotating *H. pluvialis* biofilms: From cell adhesion to maturation

For the first time, *H. pluvialis* biofilms were cultivated on cotton carriers using a rotating biofilm system, successfully reproducing the typical stages of astaxanthin production (carotenogenesis) observed

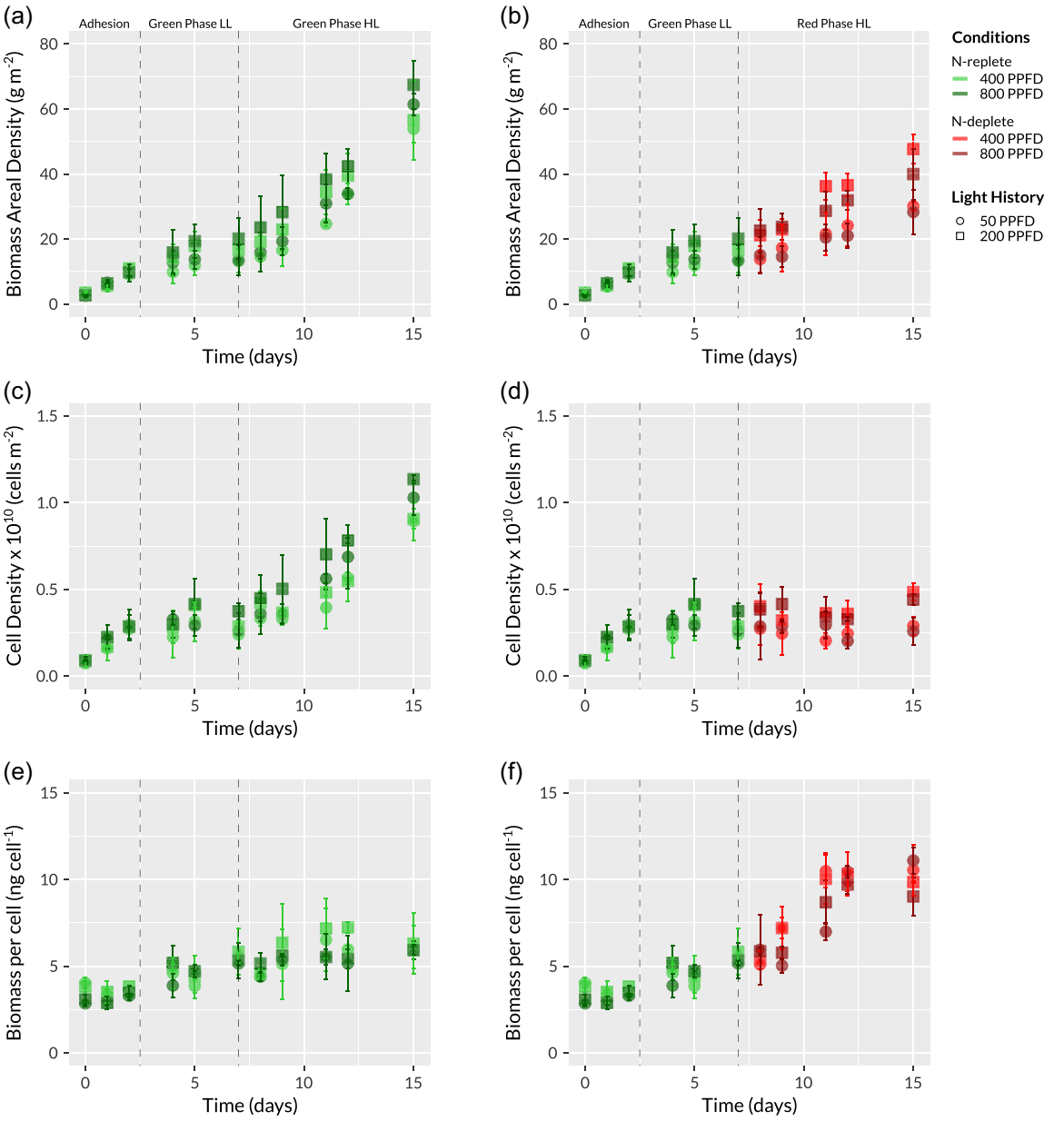

FIGURE 4 Biomass (g m^{-2}) and cell (cells m^{-2}) areal densities and biomass per cell (ng $cell^{-1}$) dynamics in *Haematococcus pluvialis* biofilms over 15 days of cultivation Biofilms growth stages (vertical dashes lines) are detailed in Table 1. On Day 7, in panels (a), (c), and (e), the biofilms were N-replete, and in panels (b), (d), and (f), the biofilms were N-deplete.

in both planktonic and biofilm-based culture technologies (Boussiba & Vonshak, 1991; Boussiba, 2000; Kiperstok et al., 2017; Zhang et al., 2017). Thanks to an in-depth characterization, the classical life cycle of biofilms reported in the state-of-the-art was identified (Sauer et al., 2022; Schnurr & Allen, 2015).

The adhesion of cells to a substrate is the first step in biofilm formation. Furthermore, the inoculum acts as a key step that can potentially introduce an additional layer of complexity into experimental designs or commercial processes (Gross et al., 2015). Indeed, previous studies have highlighted the impact of inoculum characteristics, such as cell density and light history, on subsequent biofilm maturation in both biomass and molecule productivity (Cheng et al., 2018; Li et al., 2021). Therefore, special attention must be given to the way the inoculum of the reactor is performed to ensure healthy and stable biofilm development. In biofilm-based systems, cell seeding typically employs a concentrated microalgae paste, obtained either through flocculating agents or centrifugation. This paste is then applied to the carrier material through filtration or by brushing/spraying the cells onto them (Naumann et al., 2013; Schultze et al., 2015; Zheng et al., 2019). In our study, the inoculation procedure is simpler, energy-efficient, and cost-effective. From an initial planktonic culture concentration of 0.75 g L^{-1}, a fast and uniform biomass distribution on the cotton carrier was achieved (Figure 2). Indeed, the affinity of *H. pluvialis* for cotton fabric was

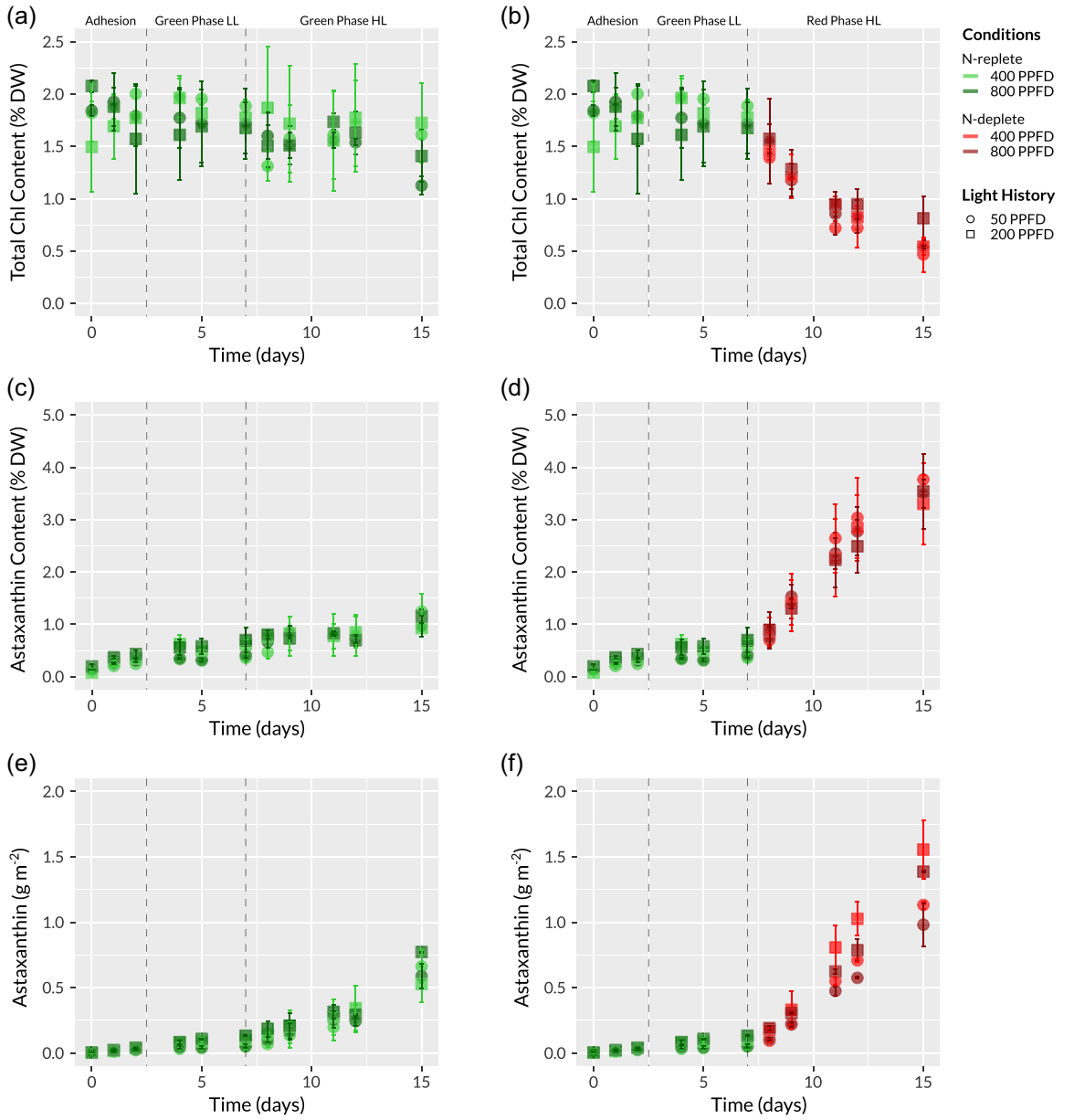

FIGURE 5 Total chlorophyll content (% DW), astaxanthin content (% DW), and astaxanthin areal density (g m^{-2}) dynamics in *Haematococcus pluvialis* biofilms over 15 days of cultivation. Biofilm growth stages (vertical dash lines) are detailed in Table 1. On Day 7, in panels (a), (c), and (e), the biofilms were N-replete, and in panels (b), (d), and (f), the biofilms were N-deplete.

notably high. Within just 4 h, the cells were collected by the rotating cylinders, achieving a biomass areal density of 3.0 ± 0.5 g m^{-2}. Interestingly, the adhesion stage followed similar dynamics, independent of light intensity. This stage was therefore attributed to the rotation of the cylinders (Figure 3).

In rotating systems, while initial adhesion is influenced by the natural ability of microalgae to attach to the substrate and by its surface's physico-chemical properties and texture, it becomes significantly easier for subsequent algal cells to attach once colonies have formed (Gross et al., 2015; Li et al., 2021; Ozkan & Berberoglu, 2013). Indeed, cell-to-substratum interactions that are often modeled using the thermodynamic DLVO, and XDLVO approaches, do not always align with observed algal adhesion behaviors due to the production of EPS (Cheah & Chan, 2021). In *H. pluvialis*, glycosidic moieties present on the cell wall during both nonmotile vegetative and cyst stages (Gutman et al., 2011), may confer to the cells a higher affinity toward cotton fibers explaining the rapid adhesion to the cotton carriers observed in this study. Corroborating this, Kiperstok et al. (2017) highlighted the exceptional biofilm-forming capabilities of the CCAC 0125 strain among several others.

Once the cells adhere to a substrate, they undergo several transitions to obtain a better fitness under immobilized conditions. In bacterial cells, this transition stage often involves a transcriptional reorganization that yields phenotypic and metabolic alterations. For

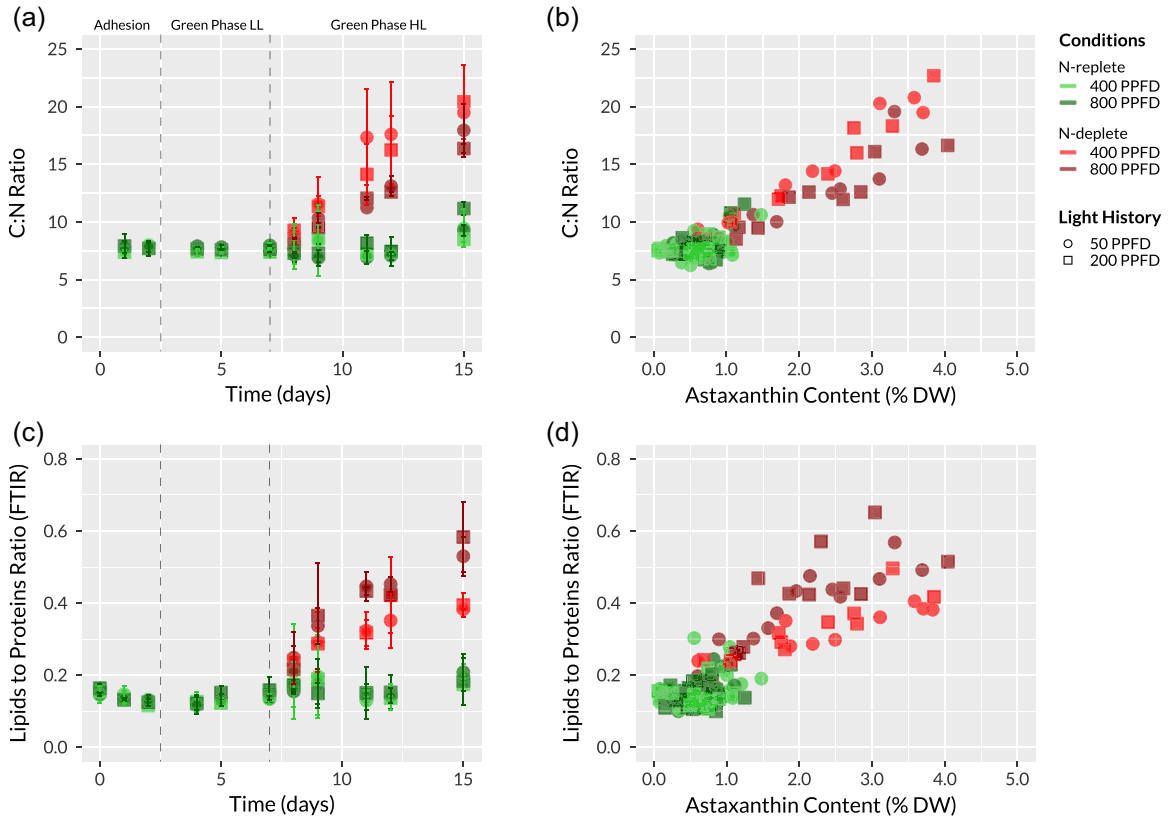

FIGURE 6 Temporal dynamics of the elemental composition (as C:N ratio) and lipids to proteins ratio in *Haematococcus pluvialis* biofilms (a and c), along with their relationships with astaxanthin content (b and d).

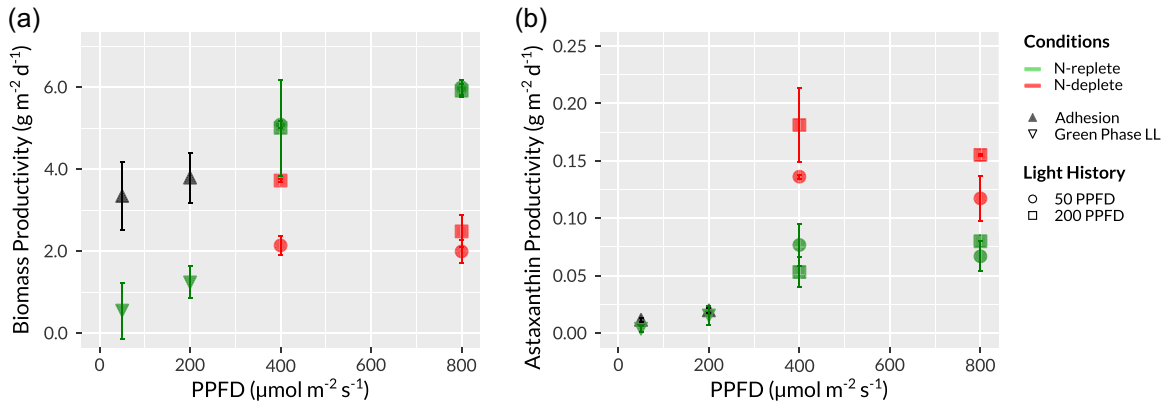

FIGURE 7 Light history effect on biomass and astaxanthin productivities in *Haematococcus pluvialis* biofilms. Biomass (a) and astaxanthin productivity (b) at different light intensities and nutrient conditions, considering the light history at which the biofilms were pre-exposed to.

instance, bacteria often lose their flagella and produce extracellular polysaccharides as stress responses, contributing to their persistence in favorable niches (Jefferson, 2004; Wu et al., 2021). Analogous behaviors have been observed in microalgae biofilms (Schnurr and Allen (2015) and references therein).

In their planktonic state, *H. pluvialis* cells are typically motile due to their pair of flagella. However, within the first 2 days post-immobilization, we primarily observed them in the nonmotile vegetative stage (Figure 2). In planktonic cultures, this shift is typically associated with the onset of an external stressor (Boussiba & Vonshak, 1991). In biofilms, the triggering factor responsible for this transition could be the change in local growth conditions accompanying the immobilized lifestyle (Li et al., 2024). Accordingly, together with the loss of motility, in this stage, the cells also started to accumulate astaxanthin, suggesting an ongoing acclimation to the new light environment (Figure 3b).

Upon adhering to a substrate, the next step in *H. pluvialis* life cycle is growth and division to further sustain biofilm maturation.

However, by Day 4, the growth rate decreased reaching a *plateau*. This suggests that the cotton carriers had saturated their biomass adsorption capacity and that the incoming photons limited further growth (Figure 3a). Interestingly, at Day 7, regardless of the presence or absence of nutrients, the higher PPFDs (400 or 800) stimulated a rapid increase in areal biomass (Figure 4a), supporting the hypothesis that the previous stage was light-limited. However, depending on the nutrient level (N-replete or N-deplete), this increase was the outcome of two different processes related to the cell cycle. Under N-replete conditions, the increase in PPFD stimulated cell division leading to a threefold increase in cell areal density, in line with the biomass areal density (Figure 4c), which maintained a stable macromolecular and elemental composition typical of balanced growth (Support Information: Table S1) (Panis & Carreon, 2016). Conversely, under the N-deplete condition, cell division ceased (stable cell densities from Day 7 onwards) (Figure 4), resulting in lipids and astaxanthin accumulation, with cells doubling in weight (Figure 4f). This is a typical response in *H. pluvialis* triggered by light or nutrient stress. Cells arrest in specific cell cycle stages and increase their volume drastically during encystment (Boussiba, 2000). It is remarkable to notice that in this condition, the different growth patterns (cell growth but no cell division) resulted in just a 20% reduction of biomass areal density, with respect to N-replete ones, despite the threefold difference in cell areal density.

From a physiological point of view, nitrogen deprivation triggers intensive carbohydrate production. These carbohydrates are later partially catabolized to support fatty acid synthesis, resulting in the formation of cytoplasmic lipid droplets which act as a repository for astaxanthin molecules (Solovchenko, 2015). This pronounced macromolecular reshuffling, especially when linked to core metabolic processes, results in noticeable changes in cellular stoichiometry. For instance, the C:N ratio increased from 7 to 22 and these changes were reflected in the FTIR spectral fingerprint of the cells (Figure 6). Our findings indicate a three- to fourfold surge in the lipids to proteins ratio, enabling us to distinguish between N-replete cells (with a ratio <0.2) and N-depleted cells (ratio >0.3). Notably, previous research has also shown that the ratio of the IR absorption band at 1740 cm^{-1} to the band at 1156 cm^{-1} can be used to identify astaxanthin hyperproducing strains (Liu & Huang, 2016). All these cellular dynamics are closely correlated with astaxanthin content (Figure 6b,d). Intriguingly, meriting further investigation, we observed distinct patterns associated with the two light intensities. For the same astaxanthin content, there is a higher lipids to proteins ratio but a lower C:N ratio for a PPFD of 800 compared to 400 (Figures 6a,c), suggesting that the partitioning of carbon and nitrogen within cells, as elucidated by Recht et al. (2012, 2014), is selectively impacted by different light intensities.

4.2 | Light history of biofilms affects astaxanthin productivity

Microalgae, either in the planktonic or in the immobilized state, are able to rapidly respond to external fluctuations by adjusting their composition and metabolic activity to perform at their best under the new conditions (Raven & Geider, 2003). The change in local external conditions related to immobilization (nutrient transport and light availability) may induce further stress on the cells, which may fail to acclimate under the new conditions. In support of this hypothesis, previous works have shown how the light history of photosynthetic biofilms strongly affects important traits such as productivity, composition, and resistance to stressors (metals, chemicals, and intense light conditions) (Bonnineau et al., 2012; Li et al., 2021). In particular, the light history of the cells may play a key role during the initial stages of immobilization. This is a crucial period when cells need to acclimate to the new environment. From another point of view, manipulating specific light histories could be strategically employed, especially when there is a need to induce conditions that stimulate the synthesis of a specific molecule to boost its productivity.

In this study, we tested how the initial light conditions used to cultivate *H. pluvialis* biofilms affect the later astaxanthin productivity in mature biofilms. Biofilms pre-exposed to relatively high light are supposed to perform better, or at least to have a shorter transitory acclimation phase, because of a smaller gap between the vegetative and induction stages. Indeed, stepwise light irradiation can result in the gradual transformation of cells to cysts and contribute to better accumulation of astaxanthin, because the cells are capable of coping with increasing levels of stress (Park et al., 2014). Interestingly, we found that the light history seemed to have an influence on various biofilm traits. When they were pre-exposed to mid-light (PPFD of 200), their biomass productivity was promoted (58.5% and 41.1% to a PPFD of 400 and 800, respectively) with respect to the biofilms pre-exposed to a PPFD of 50. Although the final astaxanthin content (as % of DW) was not directly affected by the light history, we observed higher astaxanthin productivity in the biofilms pre-exposed to a PPFD of 200 due to their higher areal biomass. We propose that inducing the transition from green to brown biofilms with mid-light (PPFD of 200) (Figure 2a) may result in higher phenotypic resistance of the cells (Figure 2c). Accordingly, nonmotile cells have been described to be more resistant to stress than vegetative cells (Han et al. (2012). In this study, this could explain the ability of the biofilms to better withstand the subsequent induction stage, leading to greater biomass and astaxanthin productivity (Figure 7). It is also possible that the immobilization itself, during biofilm formation, might induce a higher basal resistance when cells become nonmotile. Wang et al. (2014) suggested that in planktonic cultures, the transition from motile to nonmotile cells before the red-stage conditions minimizes cell mortality and may greatly enhance astaxanthin and lipid production. This strategy was also corroborated by Li et al. (2019) and must be further investigated in biofilms.

Our findings emphasize the strategic importance of light history during the green stage to enhance the productivity and resilience of a determined biofilm-based process. Interestingly, priming is nowadays being researched in plants for improving crops productivity (Liu et al., 2022), in marine macrophytes, including seagrasses and macroalgae, to become less susceptible to heat events

(Jueterbock et al., 2021) and few studies have investigated its potential on bacterial biofilms (Andrade-Linares et al., 2016; Navada et al., 2020). Our results seem to suggest that photosynthetic biofilms may possess a similar "stress memory"; however, it remains an open question whose metabolic mechanisms are behind this response.

4.3 | Rotating systems as a possible alternative to static biofilm systems

Most reported approaches for the cultivation of *H. pluvialis* biofilms, and immobilized microalgae in general, involve the use of membranes or porous substrates (PSBR) (Do et al., 2021; Kiperstok et al., 2017; Tran et al., 2019; Wan et al., 2014; Yin et al., 2015; Zhang et al., 2014). These cultivation technologies offer several advantages, including the counter gradient of light and nutrients which facilitates the production of astaxanthin in a one-stage process (Kiperstok et al., 2017). However, such systems have intrinsic limitations in terms of up-scaling (Podola et al., 2017).

Our research introduces the rotating biofilm reactor as an innovative and scalable alternative for *H. pluvialis* cultivation and astaxanthin production. While we observed productivity values comparable with previous works (Supporting Information: Table S2), the transition to a biofilm-based system is not without challenges, and several hurdles need to be addressed to establish an economically viable process.

To date, biofilm-based systems for *H. pluvialis*, including our study, have predominantly been limited to laboratory scales, with a few attempts at pilot scale (Tran et al., 2019). The results, though promising, may significantly deviate from the actual productivity achievable in outdoor environments. Also, it must be kept in mind that, the inherent difficulties associated with the scaling up of suspension photobioreactors also apply to biofilm systems. Issues related to contamination, light, and CO_2 supply, persist (Teng et al., 2023; Yu et al., 2022). However, emerging industrial rotating systems and recent LCAs point to the possibility of a growing market (Morales et al., 2020; Penaranda et al., 2023).

A critical observation is that, despite the many merits of biofilm-based systems, especially concerning biomass and astaxanthin productivity, they still did not show significant improvements over traditional planktonic cultures (Li et al., 2020). Consequently, the shift toward a biofilm approach primarily leans toward comparative cost-effectiveness and operational simplicity rather than an improvement in biological productivity (Li et al., 2020).

In this context, rotating systems might hold an edge over PSBR due to the ability to exploit the rotating mechanism to improve astaxanthin productivity. By modulating the rotational speed, light exposure can be fine-tuned during each process stage (Gao et al., 2023; Grenier et al., 2019; Grobbelaar et al., 1996), ensuring optimal conditions during both green and red stages. Additionally, exploring the rotation dynamics to introduce additional stressors, such as a controlled drought of the biofilm, may be a cost-effective strategy to induce astaxanthin synthesis for industrial applications (Boussiba, 2000; Roach et al., 2022).

The next step forward for commercial utilization hinges on the development of noninvasive monitoring tools that can provide an on-line characterization of the biofilm traits. Integrating these tools as real-time sensors, combined with research into the biofilm formation capability of other high value-added producing microalgae (Levasseur et al., 2020), could fundamentally further improve this technology. Finally, it becomes evident that additional progress in mathematical models (Bara et al., 2019; Jones et al., 2023; Zhang et al., 2016) and optimization of control strategies will be crucial to ensure that the implementation of microalgae biofilm-based technology is robust on an industrial scale.

5 | CONCLUSION

In this study, we have successfully pioneered the use of a rotating biofilm-based system for producing astaxanthin using *H. pluvialis* biofilms. We characterized biofilm traits, morphology, and structure, from adhesion to maturation, influenced by light intensity, nutrient regime, and biofilm priming.

Astaxanthin synthesis was triggered by high light intensities and N-deplete conditions, which also led to a parallel chlorophyll decline, an increase in the biomass per cell, and a higher C:N and lipids to proteins ratio. Interestingly, biofilm priming during the green stage significantly improved astaxanthin productivity.

We demonstrated the potential of using rotating systems to produce high-value compounds and the introduction of new strategies such as priming to operate them efficiently. The astaxanthin productivity in our system was comparable with that of other biofilm-based systems (PSBR), even without a targeted and dedicated system optimization, validating the proof of concept. Further advancements in monitoring, and consequent implementation of mathematical models and control strategies will be necessary for its implementation at larger scale.

AUTHOR CONTRIBUTIONS

David Morgado and Andrea Fanesi designed and performed the experiments, analyzed the data, and wrote the article. Thierry Martin built the rotating biofilm system. Filipa Lopes provided funding, supervised the project, and revised the manuscript. Sihem Tebbani and Olivier Bernard revised the article.

ACKNOWLEDGMENTS

The authors would also like to thank Hélène Santigny for her continuous technical support provided during the experiments and Vincent Butin for the CHNS analysis. This project has received funding from the European Union's Horizon 2020 Research and Innovation Program under the Marie Skłodowska-Curie grant agreement no. 955520 DigitAlgaesation.

CONFLICT OF INTEREST STATEMENT

The authors declare no conflict of interest.

DATA AVAILABILITY STATEMENT

The data that support the findings of this study are available from the corresponding author upon reasonable request.

ORCID

David Morgado http://orcid.org/0009-0006-9722-0254
Andrea Fanesi http://orcid.org/0000-0003-1410-3169
Olivier Bernard http://orcid.org/0000-0003-2539-9014
Filipa Lopes http://orcid.org/0000-0002-0156-0048

REFERENCES

Andrade-Linares, D. R., Lehmann, A., & Rillig, M. C. (2016). Microbial stress priming: A meta-analysis. *Environmental Microbiology*, *18*(4), 1277–1288. https://doi.org/10.1111/1462-2920.13223

Bara, O., Bonnefond, H., & Bernard, O. (2019). Model development and light effect on a rotating algal biofilm. *IFAC-PapersOnLine*, *52*(1), 376–381. https://doi.org/10.1016/j.ifacol.2019.06.091

Bernard, O., Lopes, F., Pruvost, E., & Sciandra, A. (2015). *Method and unit for producing microalgae*. World Intellectual Property Organization Patent WO2015007724A1. https://patents.google.com/patent/WO2015007724A1/

Berner, F., Heimann, K., & Sheehan, M. (2015). Microalgal biofilms for biomass production. *Journal of Applied Phycology*, *27*(5), 1793–1804. https://doi.org/10.1007/s10811-014-0489-x

Blanken, W., Janssen, M., Cuaresma, M., Libor, Z., Bhaiji, T., & Wijffels, R. H. (2014). Biofilm growth of *Chlorella sorokinianain* a rotating biological contactor based photobioreactor. *Biotechnology and Bioengineering*, *111*(12), 2436–2445. https://doi.org/10.1002/bit.25301

Bonnineau, C., Sague, I. G., Urrea, G., & Guasch, H. (2012). Light history modulates antioxidant and photosynthetic responses of biofilms to both natural (light) and chemical (herbicides) stressors. *Ecotoxicology*, *21*(4), 1208–1224. https://doi.org/10.1007/s10646-012-0876-5

Boussiba, S. (2000). Carotenogenesis in the green alga *Haematococcus pluvialis*: Cellular physiology and stress response. *Physiologia Plantarum*, *108*(2), 111–117. https://doi.org/10.1034/j.1399-3054.2000.108002111.x

Boussiba, S., & Vonshak, A. (1991). Astaxanthin accumulation in the green alga *Haematococcus pluvialis*. *Plant and Cell Physiology*, *32*(7), 1077–1082. https://doi.org/10.1093/oxfordjournals.pcp.a078171

Cheah, Y. T., & Chan, D. J. C. (2021). Physiology of microalgal biofilm: A review on prediction of adhesion on substrates. *Bioengineered*, *12*(1), 7577–7599. https://doi.org/10.1080/21655979.2021.1980671

Cheng, P., Wang, Y., Osei-Wusu, D., Liu, T., & Liu, D. (2018). Effects of seed age, inoculum density, and culture conditions on growth and hydrocarbon accumulation of *Botryococcus braunii* SAG807-1 with attached culture. *Bioresources and Bioprocessing*, *5*(1), 15. https://doi.org/10.1186/s40643-018-0198-4

Christenson, L. B., & Sims, R. C. (2012). Rotating algal biofilm reactor and spool harvester for wastewater treatment with biofuels by-products. *Biotechnology and Bioengineering*, *109*(7), 1674–1684. https://doi.org/10.1002/bit.24451

Conrath, U., Beckers, G. J. M., Flors, V., García-Agustín, P., Jakab, G., Mauch, F., Newman, M.-A., Pieterse, C. M. J., Poinssot, B., Pozo, M. J., Pugin, A., Schaffrath, U., Ton, J., Wendehenne, D., Zimmerli, L., & Mauch-Mani, B. (2006). Priming: Getting ready for battle. *Molecular Plant-Microbe Interactions*, *19*(10), 1062–1071. https://doi.org/10.1094/MPMI-19-1062

Do, T.-T., Ong, B.-N., Le, T.-L., Nguyen, T.-C., Tran-Thi, B.-H., Thu Hien, B. T., Melkonian, M., & Tran, H.-D. (2021). Growth of *Haematococcus pluvialis* on a Small-scale angled porous substrate photobioreactor for green stage biomass. *Applied Sciences*, *11*(4), 1788. https://doi.org/10.3390/app11041788

van Duinen, R., Rivière, C., Strosser, P., Dijkstra, J., Rios, S., Luzzi, S., Bruhn, A., Olaf Nielsen, M., Göke, C., Bhagya Samarasinghe, M., Chassé, E., Heide Nielsen, C., & Thomsen, M. (2023). *Algae and climate*. Publications Office of the European Union. https://doi.org/10.2926/208135

Elystia, S., Nasution, F. H. M., & Sasmita, A. (2023). Rotary algae biofilm reactor (RABR) using microalgae *Chlorella* sp. for tofu wastewater treatment. *Materials Today: Proceedings*, *87*, 263–271. https://doi.org/10.1016/j.matpr.2023.03.206

Fanesi, A., Paule, A., Bernard, O., Briandet, R., & Lopes, F. (2019). The architecture of monospecific microalgae biofilms. *Microorganisms*, *7*(9), 352. https://doi.org/10.3390/microorganisms7090352

Gao, Y., Bernard, O., Fanesi, A., Perré, P., & Lopes, F. (2023). The impact of light/dark regimes on structure and physiology of *Chlorella vulgaris* biofilms. *Frontiers in Microbiology*, *14*, 1250866. https://www.frontiersin.org/articles/10.3389/fmicb.2023.1250866

Grenier, J., Bonnefond, H., Lopes, F., & Bernard, O. (2019). The impact of light supply to moving photosynthetic biofilms. *Algal Research*, *44*, 101674. https://doi.org/10.1016/j.algal.2019.101674

Grobbelaar, J. U., Nedbal, L., & Tichý, V. (1996). Influence of high frequency light/dark fluctuations on photosynthetic characteristics of microalgae photoacclimated to different light intensities and implications for mass algal cultivation. *Journal of Applied Phycology*, *8*(4), 335–343. https://doi.org/10.1007/BF02178576

Gross, M., Henry, W., Michael, C., & Wen, Z. (2013). Development of a rotating algal biofilm growth system for attached microalgae growth with in situ biomass harvest. *Bioresource Technology*, *150*, 195–201. https://doi.org/10.1016/j.biortech.2013.10.016

Gross, M., Jarboe, D., & Wen, Z. (2015). Biofilm-based algal cultivation systems. *Applied Microbiology and Biotechnology*, *99*(14), 5781–5789. https://doi.org/10.1007/s00253-015-6736-5

Gross-Wen Technologies. (2014). https://algae.com/

Gutman, J., Zarka, A., & Boussiba, S. (2011). Evidence for the involvement of surface carbohydrates in the recognition of *Haematococcus pluvialis* by the parasitic blastoclad *Paraphysoderma sedebokerensis*. *Fungal Biology*, *115*(8), 803–811. https://doi.org/10.1016/j.funbio.2011.06.006

Han, D., Wang, J., Sommerfeld, M., & Hu, Q. (2012). Susceptibility and protective mechanisms of motile and non motile cells of *Haematococcus pluvialis* (Chlorophyceae) to photooxidative stress. *Journal of Phycology*, *48*(3), 693–705. https://doi.org/10.1111/j.1529-8817.2012.01147.x

Harrington, B., Gould, T., & Hursten, N. (2003). *Inkscape*. https://inkscape.org/

Inalve. (2016). https://inalve.com/en/

Jefferson, K. K. (2004). What drives bacteria to produce a biofilm? *FEMS Microbiology Letters*, *236*(2), 163–173. https://doi.org/10.1111/j.1574-6968.2004.tb09643.x

Jones, G. B., Sims, R. C., & Zhao, J. (2023). Experimental and theoretical investigations of rotating algae biofilm reactors (RABRs): Areal productivity, nutrient recovery, and energy efficiency. *Biotechnology and Bioengineering*, *120*, 2865–2879. https://doi.org/10.1002/bit.28451

Jueterbock, A., Minne, A. J. P., Cock, J. M., Coleman, M. A., Wernberg, T., Scheschonk, L., Rautenberger, R., Zhang, J., & Hu, Z.-M. (2021). Priming of marine macrophytes for enhanced restoration success and food security in future oceans. *Frontiers in Marine Science*, *8*, 658485. https://doi.org/10.3389/fmars.2021.658485

Kesaano, M., & Sims, R. C. (2014). Algal biofilm based technology for wastewater treatment. *Algal Research*, *5*, 231–240. https://doi.org/10.1016/j.algal.2014.02.003

Khan, M. I., Shin, J. H., & Kim, J. D. (2018). The promising future of microalgae: Current status, challenges, and optimization of a sustainable and renewable industry for biofuels, feed, and other products. *Microbial Cell Factories*, *17*(1), 36. https://doi.org/10.1186/s12934-018-0879-x

Kiperstok, A. C., Sebestyén, P., Podola, B., & Melkonian, M. (2017). Biofilm cultivation of *Haematococcus pluvialis* enables a highly productive one-phase process for astaxanthin production using high light intensities. *Algal Research*, *21*, 213–222. https://doi.org/10.1016/j.algal.2016.10.025

Levasseur, W., Perré, P., & Pozzobon, V. (2020). A review of high value-added molecules production by microalgae in light of the classification. *Biotechnology Advances*, *41*, 107545. https://doi.org/10.1016/j.biotechadv.2020.107545

Li, F., Cai, M., Lin, M., Huang, X., Wang, J., Ke, H., Zheng, X., Chen, D., Wang, C., Wu, S., & An, Y. (2019). Differences between motile and nonmotile cells of *Haematococcus pluvialis* in the production of astaxanthin at different light intensities. *Marine Drugs*, *17*(1), 39. https://doi.org/10.3390/md17010039

Li, S. F., Fanesi, A., Martin, T., & Lopes, F. (2024). Physiological transition of *Chlorella vulgaris* from planktonic to immobilized conditions. *Algal Research*, *77*, 103354.

Li, S. F., Fanesi, A., Martin, T., & Lopes, F. (2021). Biomass production and physiology of *Chlorella vulgaris* during the early stages of immobilized state are affected by light intensity and inoculum cell density. *Algal Research*, *59*, 102453. https://doi.org/10.1016/j.algal.2021.102453

Li, X., Wang, X., Duan, C., Yi, S., Gao, Z., Xiao, C., Agathos, S. N., Wang, G., & Li, J. (2020). Biotechnological production of astaxanthin from the microalga *Haematococcus pluvialis*. *Biotechnology Advances*, *43*, 107602. https://doi.org/10.1016/j.biotechadv.2020.107602

Li, Y., Miao, F., Geng, Y., Lu, D., Zhang, C., & Zeng, M. (2012). Accurate quantification of astaxanthin from Haematococcus crude extract spectrophotometrically. *Chinese Journal of Oceanology and Limnology*, *30*(4), 627–637. https://doi.org/10.1007/s00343-012-1217-5

Liu, H., Able, A. J., & Able, J. A. (2022). Priming crops for the future: Rewiring stress memory. *Trends in Plant Science*, *27*(7), 699–716. https://doi.org/10.1016/j.tplants.2021.11.015

Liu, J., & Huang, Q. (2016). Screening of astaxanthin-hyperproducing *Haematococcus pluvialis* using Fourier transform infrared (FT-IR) and Raman microspectroscopy. *Applied Spectroscopy*, *70*(10), 1639–1648. https://doi.org/10.1177/0003702816645605

Mantzorou, A., & Ververidis, F. (2019). Microalgal biofilms: A further step over current microalgal cultivation techniques. *Science of the Total Environment*, *651*(Pt 2), 3187–3201. https://doi.org/10.1016/j.scitotenv.2018.09.355

Morales, M., Bonnefond, H., & Bernard, O. (2020). Rotating algal biofilm versus planktonic cultivation: LCA perspective. *Journal of Cleaner Production*, *257*, 120547. https://doi.org/10.1016/j.jclepro.2020.120547

Moreno Osorio, J. H., Pollio, A., Frunzo, L., Lens, P. N. L., & Esposito, G. (2021). A review of microalgal biofilm technologies: Definition, applications, settings and analysis. *Frontiers in Chemical Engineering*, *3*, 737710. https://doi.org/10.3389/fceng.2021.737710

Moreno-Garcia, L., Adjallé, K., Barnabé, S., & Raghavan, G. S. V. (2017). Microalgae biomass production for a biorefinery system: Recent advances and the way towards sustainability. *Renewable and Sustainable Energy Reviews*, *76*, 493–506. https://doi.org/10.1016/j.rser.2017.03.024

Mousavian, Z., Safavi, M., Salehirad, A., Azizmohseni, F., Hadizadeh, M., & Mirdamadi, S. (2023). Improving biomass and carbohydrate production of microalgae in the rotating cultivation system on natural carriers. *AMB Express*, *13*(1), 39. https://doi.org/10.1186/s13568-023-01548-5

Naumann, T., Çebi, Z., Podola, B., & Melkonian, M. (2013). Growing microalgae as aquaculture feeds on twin-layers: A novel solid-state photobioreactor. *Journal of Applied Phycology*, *25*(5), 1413–1420. https://doi.org/10.1007/s10811-012-9962-6

Navada, S., Vadstein, O., Gaumet, F., Tveten, A.-K., Spanu, C., Mikkelsen, Ø., & Kolarevic, J. (2020). Biofilms remember: Osmotic stress priming as a microbial management strategy for improving salinity acclimation in nitrifying biofilms. *Water Research*, *176*, 115732. https://doi.org/10.1016/j.watres.2020.115732

Nichols, H., & Bold, H. (1973). Growth media—Freshwater. In J. R. Stein (Ed.), *Handbook of phycological methods: Culture methods and growth measurements* (pp. 7–24). Cambridge University Press.

Ozkan, A., & Berberoglu, H. (2013). Cell to substratum and cell to cell interactions of microalgae. *Colloids and Surfaces B: Biointerfaces*, *112*, 302–309. https://doi.org/10.1016/j.colsurfb.2013.08.007

Panis, G., & Carreon, J. R. (2016). Commercial astaxanthin production derived by green alga *Haematococcus pluvialis*: A microalgae process model and a techno-economic assessment all through production line. *Algal Research*, *18*, 175–190. https://doi.org/10.1016/j.algal.2016.06.007

Park, J. C., Choi, S. P., Hong, M.-E., & Sim, S. J. (2014). Enhanced astaxanthin production from microalga, *Haematococcus pluvialis* by two-stage perfusion culture with stepwise light irradiation. *Bioprocess and Biosystems Engineering*, *37*(10), 2039–2047. https://doi.org/10.1007/s00449-014-1180-y

Penaranda, D., Bonnefond, H., Guihéneuf, F., Morales, M., & Bernard, O. (2023). Life cycle assessment of an innovative rotating biofilm technology for microalgae production: An eco-design approach. *Journal of Cleaner Production*, *384*, 135600. https://doi.org/10.1016/j.jclepro.2022.135600

Podola, B., Li, T., & Melkonian, M. (2017). Porous substrate bioreactors: A paradigm shift in microalgal biotechnology. *Trends in Biotechnology*, *35*(2), 121–132. https://doi.org/10.1016/j.tibtech.2016.06.004

Raven, J. A., & Geider, R. J. (2003). Adaptation, acclimation and regulation in algal photosynthesis. In A. W. D. Larkum, S. E. Douglas & J. A. Raven (Eds.), *Photosynthesis in algae* (pp. 385–412). Springer Netherlands. https://doi.org/10.1007/978-94-007-1038-2_17

Recht, L., Töpfer, N., Batushansky, A., Sikron, N., Gibon, Y., Fait, A., Nikoloski, Z., Boussiba, S., & Zarka, A. (2014). Metabolite profiling and integrative modeling reveal metabolic constraints for carbon partitioning under nitrogen starvation in the green algae *Haematococcus pluvialis*. *Journal of Biological Chemistry*, *289*(44), 30387–30403. https://doi.org/10.1074/jbc.M114.555144

Recht, L., Zarka, A., & Boussiba, S. (2012). Patterns of carbohydrate and fatty acid changes under nitrogen starvation in the microalgae *Haematococcus pluvialis* and *Nannochloropsis* sp. *Applied Microbiology and Biotechnology*, *94*(6), 1495–1503. https://doi.org/10.1007/s00253-012-3940-4

Roach, T., Böck, N., Rittmeier, N., Arc, E., Kranner, I., & Holzinger, A. (2022). Acquisition of desiccation tolerance in *Haematococcus pluvialis* requires photosynthesis and coincides with lipid and astaxanthin accumulation. *Algal Research*, *64*, 102699. https://doi.org/10.1016/j.algal.2022.102699

Sauer, K., Stoodley, P., Goeres, D. M., Hall-Stoodley, L., Burmølle, M., Stewart, P. S., & Bjarnsholt, T. (2022). The biofilm life cycle: Expanding the conceptual model of biofilm formation. *Nature Reviews Microbiology*, *20*(10), 608–620. https://doi.org/10.1038/s41579-022-00767-0

Schneider, C. A., Rasband, W. S., & Eliceiri, K. W. (2012). NIH Image to ImageJ: 25 years of image analysis. *Nature Methods*, *9*(7), 671–675. https://doi.org/10.1038/nmeth.2089

Schnurr, P. J., & Allen, D. G. (2015). Factors affecting algae biofilm growth and lipid production: A review. *Renewable and Sustainable Energy Reviews*, *52*, 418–429. https://doi.org/10.1016/j.rser.2015.07.090

Schultze, L. K. P., Simon, M.-V., Li, T., Langenbach, D., Podola, B., & Melkonian, M. (2015). High light and carbon dioxide optimize surface productivity in a Twin-Layer biofilm photobioreactor. *Algal Research*, *8*, 37–44. https://doi.org/10.1016/j.algal.2015.01.007

Solovchenko, A. E. (2015). Recent breakthroughs in the biology of astaxanthin accumulation by microalgal cell. *Photosynthesis Research*, *125*(3), 437–449. https://doi.org/10.1007/s11120-015-0156-3

Teng, Z., Zheng, L., Yang, Z., Li, L., Zhang, Q., Li, L., Chen, W., Wang, G., & Song, L. (2023). Biomass production and astaxanthin accumulation

of *Haematococcus pluvialis* in large-scale outdoor culture based on year-round survey: Influencing factors and physiological response. *Algal Research*, *71*, 103070. https://doi.org/10.1016/j.algal.2023.103070

Tran, H.-D., Do, T.-T., Le, T.-L., Tran Nguyen, M. L., Pham, C.-H., & Melkonian, M. (2019). Cultivation of *Haematococcus pluvialis* for astaxanthin production on angled bench-scale and large-scale biofilm-based photobioreactors. *Vietnam Journal of Science, Technology and Engineering*, *61*(3), 61–70. https://doi.org/10.31276/VJSTE.61(3).61-70

Wan, M., Hou, D., Li, Y., Fan, J., Huang, J., Liang, S., Wang, W., Pan, R., Wang, J., & Li, S. (2014). The effective photoinduction of *Haematococcus pluvialis* for accumulating astaxanthin with attached cultivation. *Bioresource Technology*, *163*, 26–32. https://doi.org/10.1016/j.biortech.2014.04.017

Wang, B., Zhang, Z., Hu, Q., Sommerfeld, M., Lu, Y., & Han, D. (2014). Cellular capacities for high-light acclimation and changing lipid profiles across life cycle stages of the green alga *Haematococcus pluvialis*. *PLoS One*, *9*(9), e106679. https://doi.org/10.1371/journal.pone.0106679

Wellburn, A. R. (1994). The spectral determination of chlorophylls a and b, as well as total carotenoids, using various solvents with spectrophotometers of different resolution. *Journal of Plant Physiology*, *144*(3), 307–313. https://doi.org/10.1016/S0176-1617(11)81192-2

Wood, J. L., Takemoto, J. Y., & Sims, R. C. (2022). Rotating algae biofilm reactor for management and valorization of produced wastewater. *Frontiers in Energy Research*, *10*, 1–8. https://www.frontiersin.org/articles/10.3389/fenrg.2022.774760

Wu, Z., Wu, Y., Huang, Y., He, J., Su, P., & Feng, D. (2021). Insights into the planktonic to sessile transition in a marine biofilm-forming *Pseudoalteromonas* isolate using comparative proteomic analysis. *Aquatic Microbial Ecology*, *86*, 69–84. https://doi.org/10.3354/ame01959

Yin, S., Wang, J., Chen, L., & Liu, T. (2015). The water footprint of biofilm cultivation of *Haematococcus pluvialis* is greatly decreased by using sealed narrow chambers combined with slow aeration rate. *Biotechnology Letters*, *37*(9), 1819–1827. https://doi.org/10.1007/s10529-015-1864-7

Yu, B. S., Lee, S. Y., & Sim, S. J. (2022). Effective contamination control strategies facilitating axenic cultivation of *Haematococcus pluvialis*: Risks and challenges. *Bioresource Technology*, *344*, 126289. https://doi.org/10.1016/j.biortech.2021.126289

Zhang, C., Liu, J., & Zhang, L. (2017). Cell cycles and proliferation patterns in *haematococcus pluvialis*. *Chinese Journal of Oceanology and Limnology*, *35*(5), 1205–1211. https://doi.org/10.1007/s00343-017-6103-8

Zhang, D., Wan, M., del Rio-Chanona, E. A., Huang, J., Wang, W., Li, Y., & Vassiliadis, V. S. (2016). Dynamic modelling of *Haematococcus pluvialis* photoinduction for astaxanthin production in both attached and suspended photobioreactors. *Algal Research*, *13*, 69–78. https://doi.org/10.1016/j.algal.2015.11.019

Zhang, W., Wang, J., Wang, J., & Liu, T. (2014). Attached cultivation of *Haematococcus pluvialis* for astaxanthin production. *Bioresource Technology*, *158*, 329–335. https://doi.org/10.1016/j.biortech.2014.02.044

Zheng, Y., Huang, Y., Xia, A., Qian, F., & Wei, C. (2019). A rapid inoculation method for microalgae biofilm cultivation based on microalgae-microalgae co-flocculation and zeta-potential adjustment. *Bioresource Technology*, *278*, 272–278. https://doi.org/10.1016/j.biortech.2019.01.083

SUPPORTING INFORMATION

Additional supporting information can be found online in the Supporting Information section at the end of this article.

How to cite this article: Morgado, D., Fanesi, A., Martin, T., Tebbani, S., Bernard, O., & Lopes, F. (2023). Exploring the dynamics of astaxanthin production in *Haematococcus pluvialis* biofilms using a rotating biofilm-based system. *Biotechnology and Bioengineering*, 1–14. https://doi.org/10.1002/bit.28624